EPJ E
Soft Matter and Biological Physics
EPJ.org
your physics journal

Eur. Phys. J. E (2016) **39**: 37 DOI 10.1140/epje/i2016-16037-2

Driven binary colloidal mixture in a 2D narrow channel with hard walls

M. Ebrahim Foulaadvand and Bahareh Aghaee

edp sciences Società Italiana di Fisica Springer

Eur. Phys. J. E (2016) **39**: 37
DOI 10.1140/epje/i2016-16037-2

THE EUROPEAN PHYSICAL JOURNAL E

Regular Article

Driven binary colloidal mixture in a 2D narrow channel with hard walls

M. Ebrahim Foulaadvand[1,2,a] and Bahareh Aghaee[1]

[1] Department of Physics, University of Zanjan, P.O. Box 45196-311, Zanjan, Iran
[2] School of Nano-Science, Institute for Research in Fundamental Sciences (IPM), P.O. Box 19395-5531, Tehran, Iran

Received 4 June 2015 and Received in final form 17 February 2016
Published online: 28 March 2016 –

Abstract. We have investigated the properties of a driven equi-molar binary colloidal mixture confined to a two-dimensional narrow channel. The walls are hard and periodic boundary condition is applied along the channel. Colloidal particles perform Brownian motion in a solvent having a fixed temperature and interact with each other via a Debye-Hückel Coulombic interaction (Yukawa potential). A constant external force drives the colloids along the channel. Two species move oppositely to each other. Hydrodynamic interactions are neglected and the dynamics is assumed to be over-damped. The flow increases nonlinearly with the external force but does not exhibit a notable dependence on channel width. Above a critical driving force the system undergoes a homogeneous-to-laning transition. It is shown that the mean lane width as well as the laning order parameter increases with the channel width. The reentrance effect is observed in the narrow channel geometry.

1 Introduction

Investigations on colloidal suspensions under external force have exhibited rapid growth and strong diversification during the past decades [1–4]. Mesoscopic colloidal suspensions play a particular role as they can be both prepared and characterized in a controllable manner. The effective interaction between colloidal particles can be adjusted by changing, *e.g.*, the salt concentration in the solvent. One main motivation to study the influence of external fields is that soft matter reacts sensitively to external perturbations and manipulations. Recent investigations exploit the intriguing possibility to expose colloids to external driving fields [1, 5] and to study their non-equilibrium dynamics in a controlled way. Computer simulations, and in particular molecular dynamics simulation, have opened up new strides onto the fascinating problem of colloids under external force. The simulation results can be verified directly in experiments and can be exploited for a systematic search for new material characteristics. We know from various computer simulations [6–19], theory (dynamical density functional approach) [20] and even experiments [17,21] that a binary mixture of colloidal suspensions when driven by a constant external field (such as gravity or an electric field) can exhibit formation of particles lanes [22, 23]. Each lane contains colloids driven alike. The phenomenon is quite similar to the lane formation in pedestrian zones [24], granular systems [25] and charge-loaded surface liquid helium [26]. Lane formation can be regarded as a non-equilibrium phase transition from a homogeneous mixed state into a non-uniform state characterised by strip-like patterns of driven alike particles. Formation of lanes arises as a competition between external drive and inter-colloidal interaction forces and appears in three-dimensional model system as well [27]. Due to the existence of the hysteresis effect, the lane formation transition is frequently classified as a first order one. By now, many important aspects of driven colloidal systems are extensively studied in bulk. Recently there has been a growing interest in properties of colloidal systems, especially the types of ordering, which are under geometric confinement [28–31]. A prototype of such systems is a narrow channel which is of great interest in microfluidic applications [32]. The transport behavior of superparamagnetic colloids confined in 2D micro-channels has been investigated both experimentally and by Brownian dynamics simulations [13, 17]. Interesting features such as layer reduction, emergence of density gradient along the channel and transverse diffusion have been reported. The aim of this paper is to shed some further lights onto the problem of driven colloids in narrow constrictions and to understand the underlying physics governing these non-equilibrium processes. In particular, we wish to explore the generic effect of confinement via hard walls on layering and transport properties in $d = 2$ and its interplay with the drive on the system characteristics. It has been shown that in equilibrium 2D systems the confining wall can cause structural transition such as layering transition [33]. Here

[a] e-mail: foolad@iasbs.ac.ir

we intend to address how confinement can affect the non-equilibrium layering phase transition in a driven system. This paper has the following organisation: In sect. 2 we describe the model. We provide the simulation details as well as our simulation results in sect. 3. The paper is concluded in sect. 4.

2 Description of the problem

We consider a binary colloidal mixture comprising N colloids of types A and B. Let the number of type A and type B colloids be N_A and N_B, respectively, and for simplicity we assume $N_A = N_B = \frac{N}{2}$ unless otherwise stated (N is even). The point-like colloids are restricted to move in a two-dimensional rectangular narrow channel cell of sides L_x and $L_y (L_x \ll L_y)$. Number density is shown by $\rho = \frac{N}{S}$, where $S = L_x L_y$ is the channel area. Type number densities are denoted by $\rho_A = \frac{N_A}{S}$ and $\rho_B = \frac{N_B}{S}$ respectively. Periodic boundary condition is applied along the y direction. The channel walls which are located at $x = 0$ and $x = L_x$ are taken as hard walls [34]. The effective repulsive pair potential $V(r)$ between two colloidal particles, irrespective of their types, at an inter-particle separation r is modeled by a screened Debye-Hückel Coulombic interaction (Yukawa potential) [35,36]

$$V(r) = V_0 \sigma \exp[-\kappa(r-\sigma)]/r, \tag{1}$$

where V_0 is an energy scale, σ determines the problem length scale and κ is the inverse of Debye screening length which controls the range of interaction and can be tuned by the concentration of added salt in the colloidal solution. Naively speaking σ can be considered as the colloids diameter. This is a valid model for charge-stabilized suspensions both in two and three dimensions [37]. The colloids are suspended in a solvent with a fixed temperature T. Besides the solvent, an external force drives the colloid along the channel. We take this force to be $\mathbf{F}^{\mathrm{ext},A} = F_A \hat{j}$ and $\mathbf{F}^{\mathrm{ext},B} = F_B \hat{j}$ for types A and B, respectively. For simplicity we consider the symmetric case $F_A = -F_B = F > 0$ unless otherwise stated. In other words, the A type colloids are driven in the positive direction along the channel whereas the type B colloids are driven in the negative direction along the channel. Furthermore, the force magnitude F is taken as a constant. The dynamics of the colloids is assumed to be completely over-damped Brownian motion with hydrodynamic interactions mediated by the solvent flow neglected which is a safe approximation if the colloidal volume fraction is small. The corresponding stochastic Langevin equation for colloids trajectories reads as

$$\gamma \frac{\mathrm{d}\mathbf{r}_i}{\mathrm{d}t} = -\nabla_{\vec{r}_i} \sum_{j \neq i} V(r_{ij}) + \mathbf{F}_i^{\mathrm{ext}} + \mathbf{F}_i^{(R)}. \tag{2}$$

Here the Stokes friction constant $\gamma = 3\pi\eta\sigma$ is assumed to be the same for both A and B colloids. Note that η is the shear viscosity of the solvent fluid and $r_{ij} = |\mathbf{r}_i - \mathbf{r}_j|$. The random force $\mathbf{F}_i^{(R)}$ which describes the kicks of the solvent molecules acting onto the i-th colloidal particle is assumed to be a Gaussian white noise with zero mean $\langle \mathbf{F}_i^{(R)} \rangle = 0$ and Dirac delta-correlated in time

$$\overline{F_{i\alpha}(t) F_{j\beta}(t')} = 2k_B T \gamma \delta_{\alpha\beta} \delta_{ij} \delta(t - t'). \tag{3}$$

The subscripts α and β stand, respectively, for the Cartesian components x, y and $k_B T$ is the thermal energy. Two useful dimensionless quantities $U_0 = \frac{V_0}{k_B T}$ and $F^* = \frac{F\sigma}{k_B T}$ will be used in the paper.

3 Brownian dynamics computer simulation

We have simulated the motion of colloids according to the above dynamics in a narrow channel of width L_x. The channel length L_y is much larger than its width and periodic boundary condition is implemented along the y direction. In our simulations lengths are measured in units of σ. The colloidal mass m does not appear in our simulation due to imposing the over-damped condition in which the inertial term $m\frac{\mathrm{d}^2\mathbf{r}}{\mathrm{d}t^2}$ is neglected. We measure the time in unit of $\tau_B = \gamma\sigma^2/V_0$. In our code we have set the friction coefficient γ equal to one as it only affects the time unit. For discretisation of the Langevin equation, we have used the Ermak algorithm [38,39]. For more details, the reader is referred to [40,41] and [42,43]. Our simulation studies involve the following set of parameters: $N = 800$, $\Delta t = 0.001\tau_B$, $\kappa\sigma = 2$ and $L_y = 80\sigma$. Other parameters will be mentioned in the text. We typically run the code for 4×10^5 time steps which equals $400\tau_B$. The first twenty percent of timesteps are for relaxation towards non-equilibrium steady state and afterwards data are gathered. As for the initial condition, we randomly distribute the colloids in the channel for each run and turn off the external force. Then we simulate the motion for $t = 50\tau_B$ until the system reaches steady state. After that we turn on the external force and wait until the non-equilibrium steady state is established. Figure 1 shows some snapshots after reaching steady state.

3.1 Flow characteristics

Let us first characterise the dependence of colloidal flow on system parameters. By flow J_A we mean the time-averaged number of type A colloids which cross a fix location (in the positive direction) per unit time and per unit length along the channel width. Similar definition applies to J_B *i.e.*; the flow of type B colloids. For the symmetric case $N_A = N_B$ these two flows should be equal to each other. According to the continuity and hydrodynamics equations the flow can be written in terms of the average velocity *i.e.*; $J = \rho\langle v \rangle$ where it is understood that the $\langle v \rangle$ is density dependent. Our Brownian dynamics simulation is unable to give us the colloidal velocity due to neglecting the inertial terms $m\frac{\mathrm{d}^2\mathbf{r}}{\mathrm{d}t^2}$. However, it would be possible to define a drift velocity v_d along the external field direction as introduced in [6]:

$$v_d = \lim_{t\to\infty} \frac{\sqrt{\langle [(\mathbf{r}(t) - \mathbf{r}(0)) \cdot \hat{y}]^2 \rangle}}{t}. \tag{4}$$

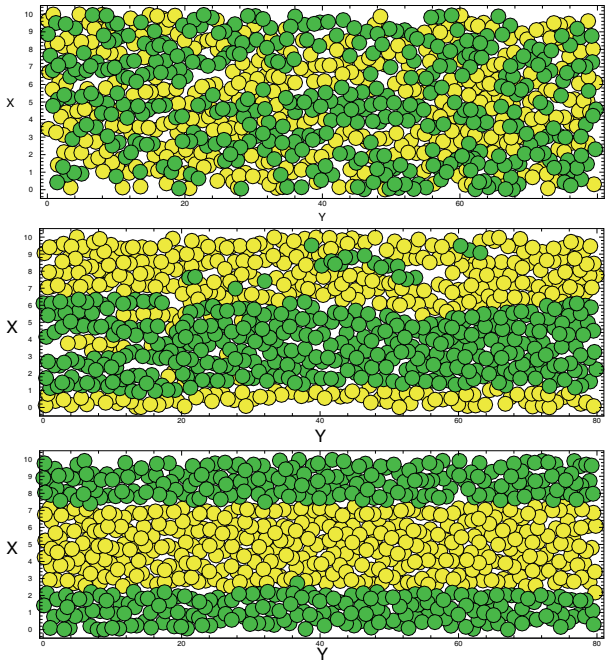

Fig. 1. System snapshots. Top: $F^* = 25$, middle: $F^* = 75$ and bottom: $F^* = 100$. The parameters are $N = 800$, $L_x = 10\sigma$, $L_y = 80\sigma$, $\rho\sigma^2 = 1$, $U_0 = 2.5$ and $\kappa\sigma = 2$.

The average can be over particles and an ensemble of runs. Figure 2 shows the dependence of J on the drive magnitude. As you see the dependence is linear for large F^* which is expected. When the driving force is larger than the other forces the colloids behave like a damped system of particles under the influence of a constant force. In this case the dynamics will no longer be over-damped. Neglecting the inter-colloidal forces which are of the order $\frac{V_0}{\sigma}$ and the thermal noise which is of order $\sqrt{k_B T\gamma}$, in comparison to F the dominant remaining force will be the frictional force γv. Hence the equation of motion in high driving limit becomes

$$m\frac{\mathrm{d}\mathbf{v}}{\mathrm{d}t} + \gamma\mathbf{v} = \mathbf{F}. \tag{5}$$

In the steady state we set $\frac{\mathrm{d}\mathbf{v}_s}{\mathrm{d}t} = 0$ and find $\mathbf{v}_s \propto \mathbf{F}$. This gives rise to an average linear velocity (and hence the flow) with respect to driving force. The effect is quite similar to the Drude model for a free electron gas in a solid where the effect of collisions can be modeled by a frictional damping term in the equations of motion [44]. Note that when F^* is small we have a non-linear flow dependence on F^*.

According to our simulation results the flow does not notably depend on the channel width L_x for various values of the driving force. Figure 3 exhibits the flow dependence on colloidal dimensionless density $\rho^* = \rho\sigma^2$. One can observe that for small densities there is a linear increasing behaviour up to $\rho^* = 2.5$. Afterwards, the flow again increases linearly with density but with a smaller slope. A qualitative explanation is in order: flow is the number of colloids times their average velocity. At low densities, flow increases with density because the number of colloids increases but the average velocity does not show a significant dependence on density. However, when the number of colloids exceeds a threshold, the interaction among them will be such as to decrease their mean velocity. A further density increment yields a reduction of the average velocity and this overally gives rise to a decrease of the flow increment rate with density in comparison to the low density regime [45].

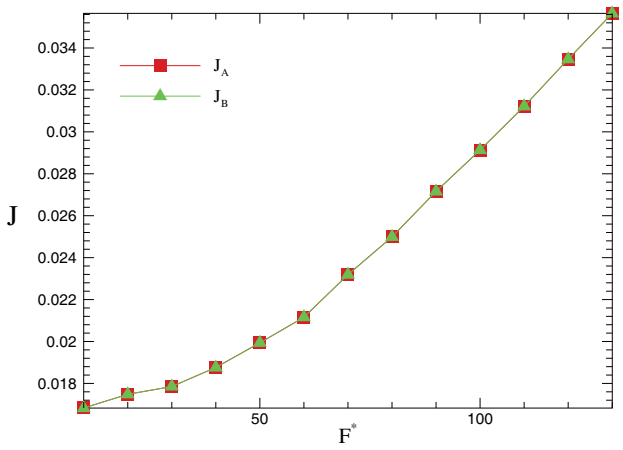

Fig. 2. Flow dependence on F^*. Parameters are $N = 800$, $L_x = 10\sigma$, $L_y = 80\sigma$, $\rho\sigma^2 = 1$, $U_0 = 2.5$, and $\kappa\sigma = 2$.

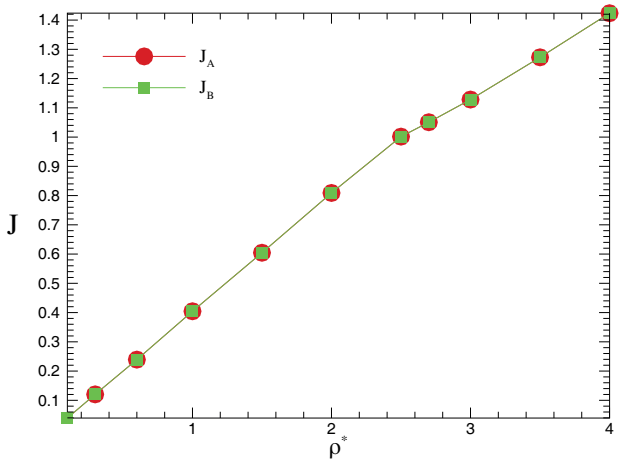

Fig. 3. Flow dependence on density ρ^*. Other parameters are $N = 800$, $L_x = 10\sigma$, $F^* = 80$, $U_0 = 2.5$, and $\kappa\sigma = 2$.

3.2 Laning order parameter

To quantify lane formation we need a suitable order parameter. Such a parameter is not unique. Two choices have been introduced in the literature [6,14]. Let us first recall the global laning parameter Φ introduced by Dzubiella *et al.* [6]. To each colloid i we assign a binary-valued order parameter ϕ_i. This quantity is one if the lateral distance $|x_i - x_j|$ between colloid i and all other colloids $j (j \neq i)$ of different type is larger than a length scale b. Otherwise ϕ_i is set to zero. The length scale b can be density dependent and was taken to be $1/(2\sqrt{\rho})$ in [6]. A global dimensionless

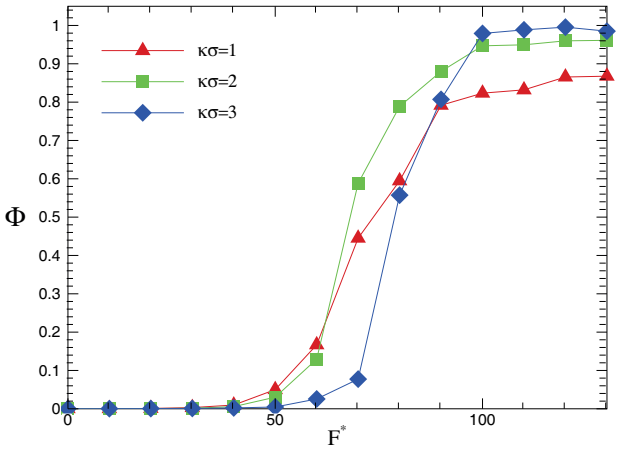

Fig. 4. Dependence of the laning order parameter Φ on driving force F^* for various values of κ. Other parameters are $N = 800$, $L_x = 10\sigma$, $L_y = 80\sigma$, $\rho\sigma^2 = 1$ and $U_0 = 2.5$.

laning order parameter can be defined as follows:

$$\Phi = \frac{1}{N}\sum_{i=1}^{N}\overline{\phi_i}, \tag{6}$$

where the over-line denotes time averaging. In a fully mixed state, the order parameter Φ becomes zero whereas in a lane-ordered phase it can be as large as one. In fig. 4 we have shown the dependence of Φ on the dimensionless force F^* for various values of κ. As you see, for small driving force we have a small Φ. For large enough driving force the laning parameter Φ approaches unity as expected. Laning parameter transition from small values to large ones is quite sharp and we expect it to be first order in the large system limit. As you can see, the transition driving force F_c^* shows a notable dependence on the inverse of Debye screening length κ. When κ is increased the critical F^* increases as well. A physical explanation can be given as follows. When κ is increased the inter-colloidal Coulombic interaction range decreases. This means that the colloids motion is more influenced by thermal fluctuations. Therefore, we need a larger force to organise them into lanes.

Our simulations show that the nature of laning in a narrow channel is quite different from the case where colloids are not spatially restricted. In non-restricted geometries the lanes are normally thin and have a wide range of width [6] but in our restricted geometry and in the channel width interval that we investigated only a few lanes are formed. Typically a single lane forms in the middle where two other lanes corresponding to the opposite species encompass it (see fig. 1). Another typical situation consists of two lanes (one for each species). See fig. 5.

It is expected that, by increasing the channel width L_x the single formed lane splits into a number of thinner width lanes. Figure 6 exhibits the dependence of the mean major lane width on the channel width L_x. As you can see the larger the channel width the larger the mean lane width. Unfortunately we could not find any results on

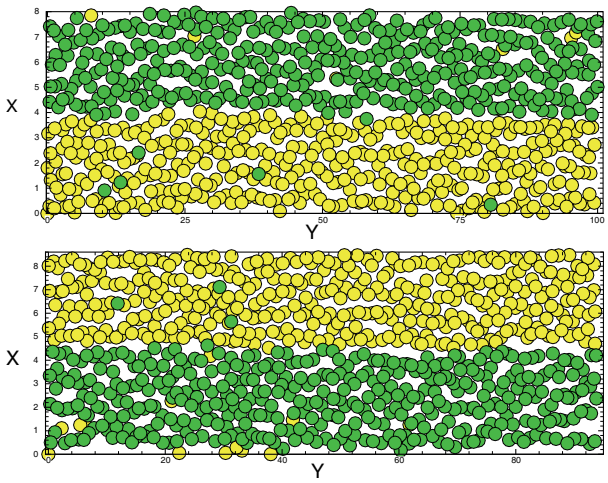

Fig. 5. System snapshots. Top: $F^* = 75$, bottom: $F^* = 100$. The parameters are $N = 800$, $L_x = 8\sigma$, $L_y = 80\sigma$, $\rho\sigma^2 = 1$, $U_0 = 2.5$ and $\kappa\sigma = 2$.

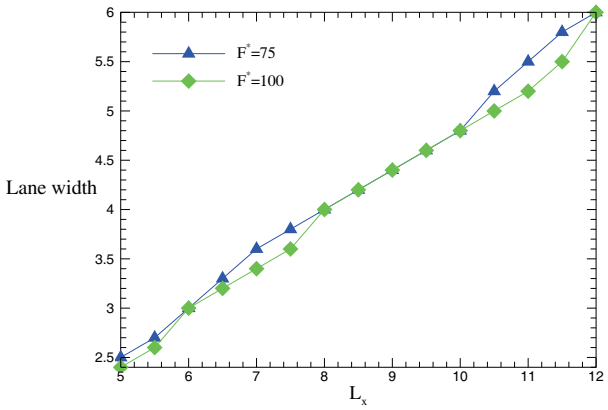

Fig. 6. Dependence of mean major lane width on the channel width L_x for two values of F^*. Other parameters are $\rho\sigma^2 = 1$, $U_0 = 2.5$, and $\kappa\sigma = 1$.

the statistics of lanes width in the non-restricted systems hence we are unable to compare our findings with bulk.

We believe that the nature of wall-particle interaction can significantly affect the laning behaviour. In fig. 7 we have sketched the dependence of Φ on the channel width L_x for various values of the driving force as well as inter-colloidal interaction constant U_0. In the top diagram and for small driving force, there is a slight increase with respect to channel width. For intermediate $F^* = 75$ we see an increasing dependence on L_x modulated with weak oscillations. When F^* is increased to a larger value $F^* = 100$ the dependence on channel width becomes weaker again. However, the weak oscillatory modulations persist. In the bottom diagram the dependence of Φ on L_x exhibits a notable dependence on the strength of inter-colloidal interaction. Weak oscillatory behaviours are yet present.

Figure 8 exhibits how Φ behaves when colloidal density ρ is varied. For small densities the inter-colloidal repulsive force, which favours a disordered state, wins the competition with the driving force therefore the system remains disordered. When the density reaches a critical value ρ_c

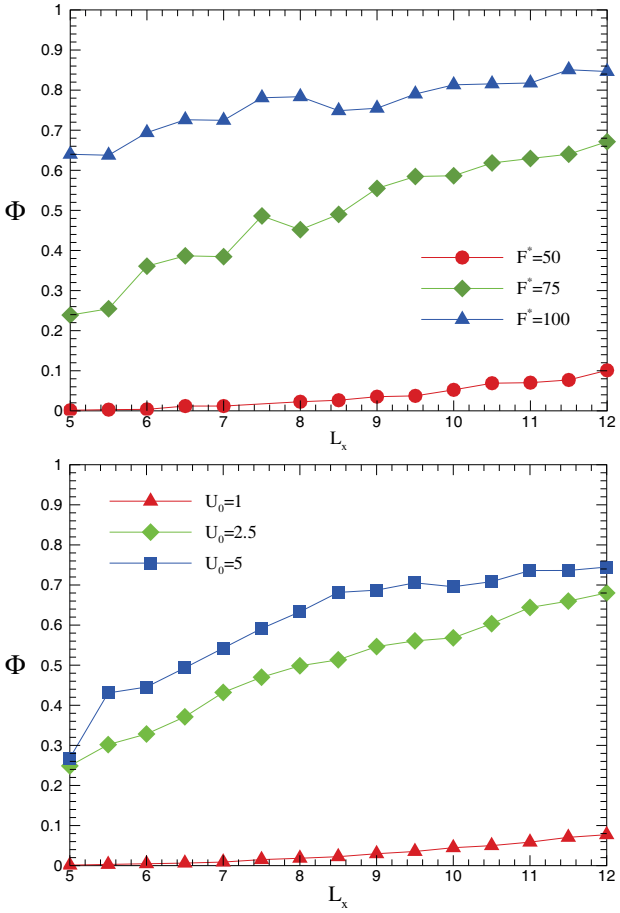

Fig. 7. Dependence of laning order parameter Φ on channel width L_x (in unit of σ). Top: for various values of driving force at $\kappa\sigma = 1$. Bottom: For various values of U_0 at $F^* = 75$. Other parameters are $N = 800$, $\rho\sigma^2 = 1$.

the driving force manages to overcome the entropic effects and succeeds in organising the colloids into lanes. For higher densities the inter-particle forces become dominant again and destroy the laning order. This is the so-called *reentrance effect* introduced in [11]. In fact, a driven binary mixture of colloids in a narrow channel undergoes reentrant effect: for a fixed high driving force there is first a transition towards laning which is followed by a back transition to the isotropic state having no lane.

We could not find a similar result for the bulk in the literature hence we are unable to compare our results with the non-restricted systems. In ref. [11] the dependence of the critical laning force F_c^* on the colloidal density is investigated. Let us next discuss the second laning order parameter which was introduce by Rex and Löwen [14]. For the sake of completeness, let us redefine this order parameter. To each colloid i we assign two numbers $n_l^i(t)$ and $n_o^i(t)$. The first one denotes the number of its same type lateral neighbours and the second one shows the number of its opposite type lateral neighbours at time t. A colloid j is a lateral neighbour of colloid i provided their lateral distance $|x_i - x_j|$ is less than a length z_L. In our simulation we set $z_L = 2\sigma$. Then a local real-valued laning

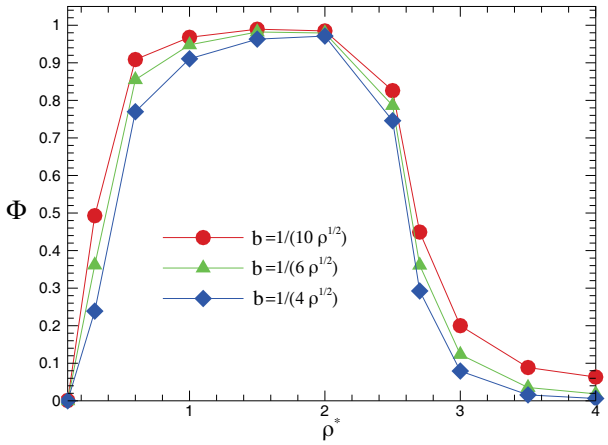

Fig. 8. Dependence of Φ on ρ^*. Other parameters: $N = 800$, $L_x = 10\sigma$, $U_0 = 2.5$, $F^* = 100$ and $\kappa\sigma = 2$.

parameters $\psi_i(t)$ is defines as follows:

$$\psi_i(t) = \frac{[n_l^i(t) - n_o^i(t)]^2}{[n_l^i(t) + n_o^i(t)]^2}. \tag{7}$$

Eventually the global lane transition order parameter Ψ is defined as follows [14]:

$$\Psi = \frac{1}{N}\sum_{i=1}^{N}\overline{\psi_i}, \tag{8}$$

where the over-line denotes time averaging. The global order parameter Ψ is practically zero for a homogeneous mixed configuration, since colloids of different types will be found inside the neighbouring distance with equal probability but it gets close to unity if the same colloids are located in the vicinity of each other, *i.e.*, in a state of lanes. Figure 9 exhibits the dependence of Ψ on the driving force F^* for various values of κ. As you can see, by increasing the driving force there is a laning transition. With respect to the laning order parameter, Ψ shows a smoother behaviour when F^* is increased. This can be related to the nature of lanes which are wide.

3.3 Soft interaction with one of the walls

In order to enhance our understanding of the lanes nature, we have also considered the case where one of the walls (the wall located at $x = 0$) exerts and extra force on type A colloids. Specifically this wall exerts a repulsive force on A colloids according to the potential $V_{\text{soft}} = U_0^{(w)}(\frac{\sigma}{r})^3$. Figure 10 shows the dependence of the laning parameter Φ on the driving force for two values of wall-colloid potential constant $U_0^{(w)}$. Comparison with the case where no soft potential exists between the $x = 0$ wall and A colloids is also made.

As you can observe, the implementation of this sort of interaction notably enhances the laning effect. The larger the potential constant $U_0^{(w)}$ the greater the order parameter.

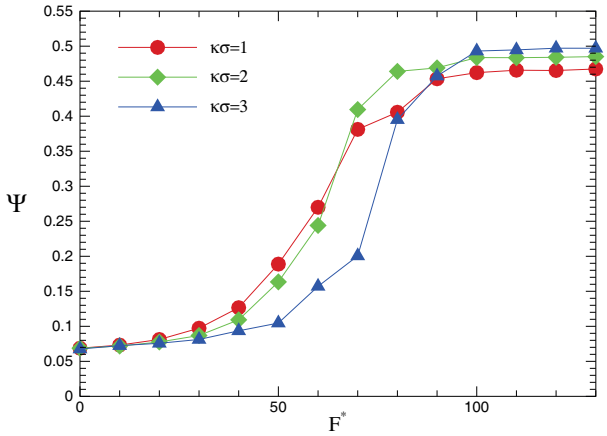

Fig. 9. Dependence of Ψ on F^*. Other parameters are $N = 800$, $L_x = 10\sigma$, $L_y = 80\sigma$, $\rho\sigma^2 = 1$ and $U_0 = 2.5$.

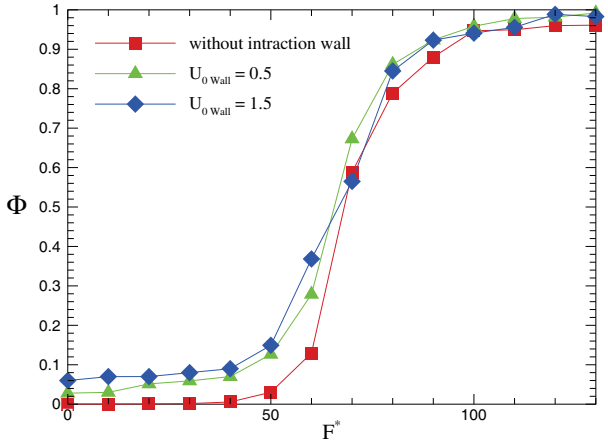

Fig. 10. Dependence of Φ on F^* with an extra soft potential between the left wall ($x = 0$) and type A colloids. Other parameters are $N = 800$, $L_x = 10\sigma$, $L_y = 80\sigma$, $\rho\sigma^2 = 1$, $U_0 = 2.5$, and $\kappa\sigma = 2$.

4 Concluding remarks

We have simulated a 2D driven binary colloidal mixture immersed in a host fluid having a fixed temperature with Brownian dynamics. Hydrodynamic interactions are neglected and over-damped approximation is adopted in the Langevin equation of motion. Colloidal species interact via a repulsive screened Coulombic potential (Yukawa potential) and move oppositely when a constant external force is exerted to them. The channel walls are assumed to be hard and the elastic collision rule models the wall-particle interaction. The colloidal current increases with external force but does not show a significant dependence on channel width. We observe the laning transition above a critical external force. The nature of the formed lanes is quite different from the case of non-restricted geometries. The mean lane width dependence exhibits an increasing behaviour with channel width modulated by weak variations. By increasing the Debye screening length, the critical external force decreases. The laning order parameter shows a notable dependence on the strength of the Yukawa potential. Similar to non-restricted geometries, a reentrant effect is observed. The effect of inclusion of an additional soft repulsive potential between one of the walls and species is investigated and it is shown that this additional force enhances the laning.

We highly wish to acknowledge the *Grid Computing Group* of the Institute for Research in fundamental Sciences (IPM) for providing us with the computational facilities. Final computational stage s of the work were supported by the IPM School of computer. We greatly appreciate this support and in particular we thank Armin Ahmadzadeh. We would like to express our gratitude to Joachim Dzubiella, Hartmut Lowen, Mike Allen, Tobias Glanz, Nadine Schwiertz and Azadeh Saeidi for fruitful discussions and comments. We are indebted to Ehsaan Nedaee from IASBS, Abbas Montazeri from Khajeh Nasir University and Abol Khosh from University of Zanjan for enlightening comments.

References

1. H. Löwen, J. Phys.: Condens. Matter **13**, R415 (2001).
2. J.K.G. Dhont, *An Introduction to Dynamics of Colloids* (Elsevier, Amsterdam, 1996).
3. C. Reichhardt, C.J. Olson Reichhardt, Phys. Rev. E **74**, 011403 (2006).
4. A. Nikoubashman, C.N. Likos, G. Kahl, Soft Matter **9**, 2603 (2013).
5. M. Sullivan, K. Zhao, C. Harrison, R.H. Austin, M. Megens, A. Hollingsworth, W.B. Russel, Z.D. Cheng, T. Mason, P.M. Chaikin, J. Phys.: Condens. Matter **15**, S11 (2003).
6. J. Dzubiella, G.P. Hoffmann, H. Löwen, Phys. Rev. E **65**, 021402 (2002).
7. J. Dzubiella, H. Löwen, J. Phys.: Condens. Matter **14**, 9383 (2002).
8. H. Löwen, J. Dzubiella, Farady Discuss. **123**, 99 (2003).
9. R.R. Netz, Europhys. Lett. **65**, 616 (2003).
10. R.B. Pandey, J.F. Gettrust, R. Seyfarth, L.A. Cueva-Parra, Int. J. Mod. Phys. C **14**, 955 (2003).
11. J. Chakrabarti, J. Dzubiella, H. Löwen, Phys. Rev. E **70**, 012401 (2004).
12. J. Delhommelle, Phys. Rev. E **71**, 016705 (2005).
13. M. Köppl, P. Henseler, A. Erbe, P. Nielaba, P. Leiderer, Phys. Rev. Lett. **97**, 208302 (2006).
14. M. Rex, H. Löwen, Phys. Rev. E **75**, 051402 (2007).
15. M. Rex, H. Löwen, Eur. Phys. J. E **26**, 143 (2008).
16. D.V. Tkachenko, V.R. Misko, F.M. Peeters, Phys. Rev. E **80**, 051401 (2009).
17. P. Henseler, A. Erbe, M. Köppl, P. Leiderer, P. Nielab, Phys. Rev. E **81**, 041402 (2010).
18. N. Schwierz, P. Nielaba, Phys. Rev. E **82**, 031401 (2010).
19. T. Glanz, H. Löwen, J. Phys.: Condens. Matter **24**, 464114 (2012).
20. J. Chakrabarti, J. Dzubiella, H. Löwen, Europhys. Lett. **61**, 415 (2003).
21. M.E. Leunissen, C.G. Christova, A.P. Hynninen, C.P. Royall, A.I. Campbell, A. Imhof, M. Dijkstra, R. van Roij, A. van Blaaderen, Nature (London) **437**, 235 (2005).
22. S.B. Santra, S. Schwarzer, H. Herrmann, Phys. Rev. E **54**, 5066 (1996).

23. P. Valiveti, D.L. Koch, Phys. Fluids **11**, 3283 (1999).
24. R. Jiang, D. Helbing, P.K. Shukla, Q.S. Wu, Physica A **368**, 567 (2006).
25. M.P. Ciamarra, A. Coniglio, M. Nicodemi, Phys. Rev. Lett. **94**, 188001 (2005).
26. P. Glasson, V. Dotsenko, P. Fozooni, M.J. Lea, W. Bailey, G. Papageorgiou, S.E. Andresen, A. Kristensen, Phys. Rev. Lett. **87**, 176802 (2001).
27. D. Wilms *et al.*, J. Phys.: Condens. Matter **24**, 464119 (2012).
28. Haghgooie, P.S. Doyle, Phys. Rev. E **70**, 061408 (2004).
29. A. Ricci, P. Nielaba, S. Sengupta, K. Binder, Phys. Rev. E **75**, 011405 (2007).
30. M.E. Foulaadvand, N. Ojaghlou, Phys. Rev. E **86**, 021405 (2012).
31. M.E. Foulaadvand, M.M. Shafiee, Eur. Phys. Lett. **104**, 30002 (2013).
32. T.M. Squires, S.R. Quake, Rev. Mod. Phys. **77**, 977 (2005).
33. D. Chaudhuri, S. Sengupta, J. Chem. Phys. **128**, 194702 (2008).
34. D.M. Heyes, J.R. Melrose, J. Non-Newtonian Fluid Mech. **46**, 1 (1993).
35. P.N. Pusey, in *Liquids, Freezing and the Glass Transition*, edited by J.P. Hansen *et al.* (North Holland, Amsterdam, 1991).
36. C.P. Royall, M.E. Leunissen, A.P. Hynninen, M. Dijkstra, A. van Blaaderen, J. Chem. Phys. **124**, 244706 (2006).
37. H. Löwen, J. Phys.: Condens. Matter **4**, 10105 (1992).
38. Donald E. Ermak, J. Chem. Phys. **62**, 4189 (1975).
39. Donald E. Ermak, J. Chem. Phys. **62**, 4197 (1975).
40. M.P. Allen, D.J. Tildesly, in *Computer Simulation of Liquids* (Clarendon Press, Oxford, 1987).
41. M.P. Allen, D. Quigley, Mol. Phys. **111**, 3442 (2013).
42. G.P. Hoffmann, H. Löwen, Phys. Rev. E **60**, 3009 (1999).
43. G.P. Hoffmann, H. Lowen, J. Phys.: Condens. Matter **12**, 7359 (2000).
44. Neil W. Ashkroft, N. David Mermin, *Solid State Physics* (Harcourt College Publisher, 1976).
45. Y. Jamali, M.E. Foulaadvand, H. Rafii-Tabar, J. Comput. Theor. Nanosci. **7**, 146 (2010).